Low Temperature Physics/Fizika Nizkikh Temperatur, 2016, v. 42, No. 7, pp. 694–698

UV-VUV synchrotron radiation spectroscopy of $NiWO_4$

A. Kuzmin[1], V. Pankratov[1,2], A. Kalinko[1,3], A. Kotlov[3], L. Shirmane,[1] and A.I. Popov[1]

[1]*Institute of Solid State Physics, University of Latvia, 8 Kengaraga str., LV-1063 Riga, Latvia*
E-mail: a.kuzmin@cfi.lu.lv

[2]*Research Center of Molecular Materials, University of Oulu, P.O. Box 3000, FIN-90014, Finland*

[3]*DESY Photon Science, Notkestraße 85, D-22607 Hamburg, Germany*

Received January 18, 2016, published online May 25, 2016

Photoluminescence and excitation spectra of microcrystalline and nanocrystalline nickel tungstate ($NiWO_4$) were measured using UV-VUV synchrotron radiation source. The origin of the bands is interpreted using comparative analysis with isostructural $ZnWO_4$ tungstate and based on the results of recent first-principles band structure calculations. The influence of the local atomic structure relaxation and of Ni^{2+} intra-ion *d–d* transitions on the photoluminescence band intensity are discussed.

PACS: 78.55.Hx Other solid inorganic materials;
61.05.cj Electron density of states and band structure of crystalline solids;
71.20.–b X-ray absorption spectroscopy: EXAFS, NEXAFS, XANES, etc.

Keywords: $NiWO_4$, $ZnWO_4$, UV-VUV spectroscopy, EXAFS, first-principles calculations.

Introduction

Metal tungstates (MWO_4) have received considerable interest from both theoretical and technological point of view due to their excellent combination of the optical, piezoelectric, ferroelectric and other properties [1,2]. The optical properties of different metal tungstates can be controlled by their composition and many wide band-gap tungstates are found to be promising materials for scintillator applications [3–10].

Among them, nickel tungstate ($NiWO_4$) finds applications in catalysis [11–14], as humidity [15] and gas [16] sensor, a photoanode in photovoltaic electrochemical cell [17], a pigment [18] and in microwave [19] and electrochromic [20,21] devices. These applications are tightly connected to its electronic structure being scarcely studied in the past. The electronic band structure of $NiWO_4$ was calculated recently using first-principles spin-polarized periodic linear combination of atomic orbitals (LCAO) method in [22]. The photoluminescence properties of $NiWO_4$ powder and sol-gel derived $NiWO_4$ films, calcined above 600°C, were investigated at room temperature under pulsed Xenon discharge lamp excitation in [23], indicating the presence of a broad blue-green (2.07–3.54 eV) photoluminescence band.

In this work we present original results on the photoluminescence and excitation spectra of microcrystalline and nanocrystalline $NiWO_4$, obtained using UV-VUV synchrotron radiation spectroscopy. The experiments were carried out at SUPERLUMI beamline (HASYLAB at DESY, Hamburg) using 4–20 eV synchrotron radiation from the DORIS storage ring for excitation [24]. This experimental set-up is a unique tool for investigations of different types of wide band gap materials [24–33]. The interpretation of the photoluminescence and excitation spectra is given based on the comparative analysis with isomorphous $ZnWO_4$ tungstate [32] and using the results of LCAO calculations [22] and the Ni(Zn) *K*-edge and W L_3-edge x-ray absorption spectroscopy studies.

Experimental and calculation details

$NiWO_4$ and $ZnWO_4$ powders were synthesized using co-precipitation technique by mixing two aqueous solutions of $Na_2WO_4{\cdot}2H_2O$ and $Ni(NO_3)_2{\cdot}6H_2O$ or $ZnSO_4{\cdot}7H_2O$ salts in bi-distilled water at room temperature (20 °C). The pH value of the solution was equal to eight. The tungstate sediment was subsequently washed, filtrated and, after drying, annealed in air for 4 h at 80 °C (nanocrystalline sample with crystallites size below 2 nm) and 900 °C (microcrystalline sample). More details can be found in [32].

The photoluminescence (Fig. 1) and excitation (Fig. 2) spectra were collected at 7–300 K exploiting ultraviolet (UV) and vacuum ultraviolet (VUV) synchrotron radiation

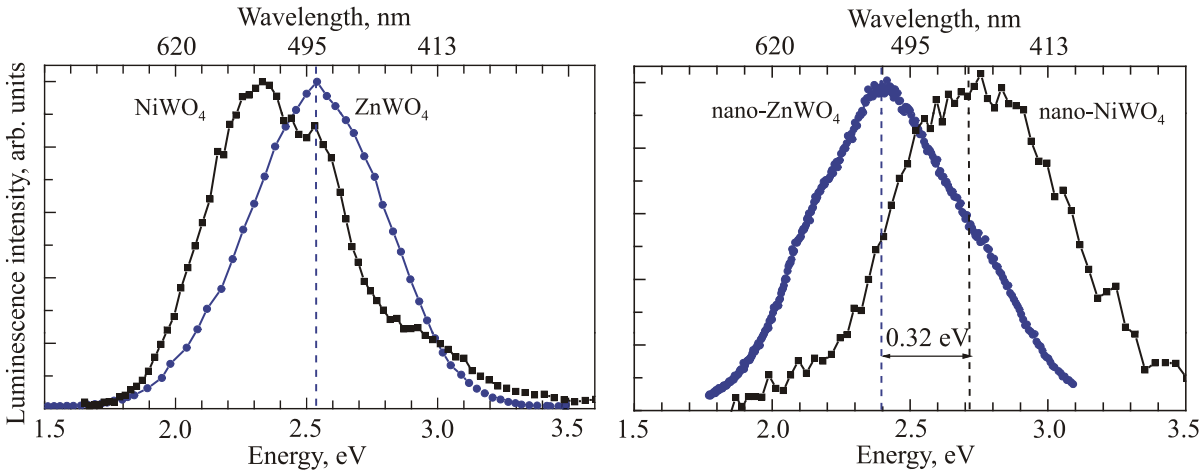

Fig. 1. The photoluminescence spectra of microcrystalline (left panel) and nanocrystalline (right panel) Ni(Zn)WO_4 powders excited by 13.8 eV photons.

(3.6–20.0 eV) emitted from DORIS III storage ring at SUPERLUMI station (HASYLAB DESY, Hamburg).

The low-temperature (10 K) Ni(Zn) *K*-edge and W L_3-edge x-ray absorption spectra were measured in transmission mode at the HASYLAB/DESY C bending-magnet beamline. The x-ray radiation was monochromatized by a detuned Si(111) double-crystal monochromator, and the beam intensity was measured using two ionization chambers filled with argon and krypton gases. The x-ray absorption spectra were analyzed using the EDA software package [34] following conventional procedure [35]. Radial distribution functions (RDFs) $G(R)$ (Fig. 3) for

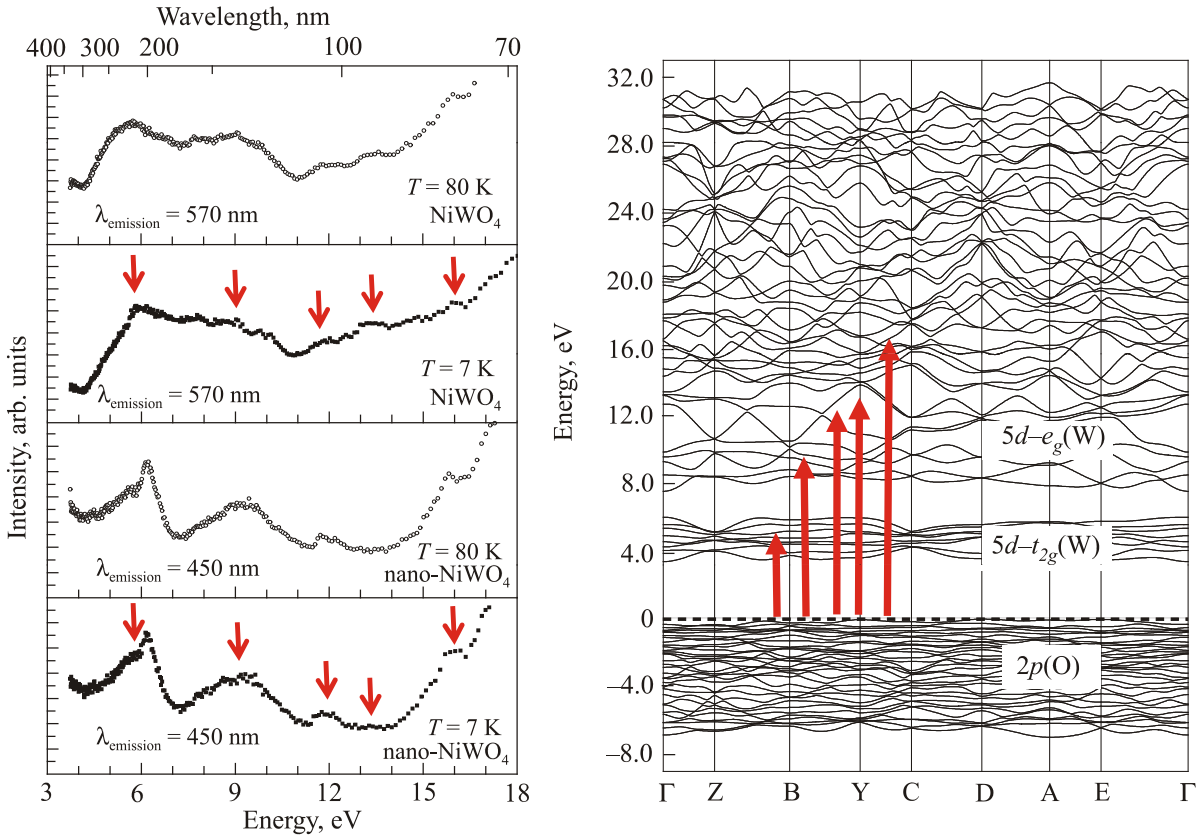

Fig. 2. Left panel: Excitation spectra of microcrystalline and nanocrystalline $NiWO_4$ at T = 7 and 80 K. The bands due to the one-electron transitions are indicated by vertical arrows. Right panel: Electronic band structure diagram for wolframite-type $NiWO_4$ from [22]. The energy zero is set at the Fermi-energy level. The one-electron transitions, corresponding to the peaks at 6, 9, 12, 13.5 and 16 eV in the excitation spectrum of $NiWO_4$ are indicated by vertical arrows.

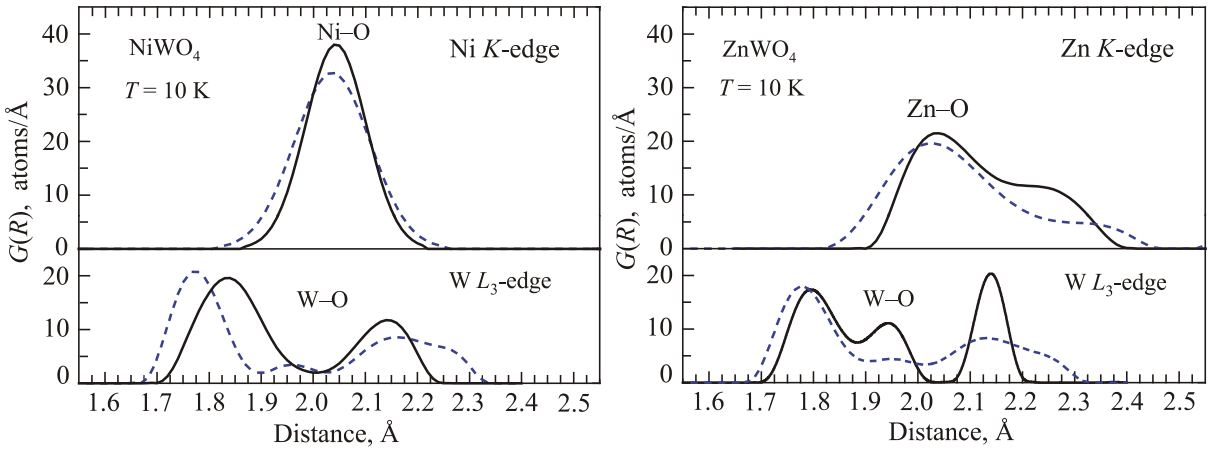

Fig. 3. Radial distribution functions (RDFs) $G(R)$ for Ni(Zn)–O and W–O bonds within the first coordination shells of metal atoms in microcrystalline (solid lines) and nanocrystalline (dashed lines) $Ni(Zn)WO_4$, obtained from the analysis of the Ni(Zn) K-edge and W L_3-edge EXAFS spectra at 10 K.

Ni(Zn)–O and W–O bonds in microcrystalline and nanocrystalline $Ni(Zn)WO_4$ were obtained by the regularization-like method [34,36,37] from the Ni(Zn) K-edge and W L_3-edge extended x-ray absorption fine structure (EXAFS) spectra. Theoretical scattering amplitude and phase shift functions, employed in the EXAFS simulations, were calculated for $NiWO_4$ and $ZnWO_4$ crystallographic structures by the *ab initio* FEFF8 code [38,39] using complex exchange-correlation Hedin–Lundqvist potential.

Results and discussion

Photoluminescence spectra

Both tungstates $NiWO_4$ and $ZnWO_4$ have monoclinic wolframite-type structure (space group $P2/c$) with two formula units ($Z = 2$) per primitive cell [40]. All metal atoms (Ni, Zn and W) are six-fold octahedrally coordinated by oxygen atoms. The presence of two non-equivalent oxygen atoms results in metal-oxygen octahedron distortion [41], which is the largest for WO_6 octahedron and the smallest for NiO_6 octahedron (Fig. 3).

The photoluminescence spectrum of microcrystalline $ZnWO_4$ powders consists of a broad band, peaked at about 2.5 eV (Fig. 1). The origin of the band has been previously assigned to radiative electron transitions within the $[WO_6]^{6-}$ molecular complex [42,43]. In $NiWO_4$, the same photoluminescence band has irregular asymmetric shape, which is close to that observed previously in solid solutions $Zn_cNi_{1-c}WO_4$ [32]. The origin of such band shape can be attributed [32] to the self-absorption effect, i.e., to a modulation of optical absorption by the intense intra-ion transition within Ni^{2+} ($3d^8$) ions from the ground state $^3A_{2g}$ to the excited state $^3T_1$ [44].

The maximum of the photoluminescence band in nano-$NiWO_4$ is located at 2.7 eV, thus being shifted by ~0.32 eV to higher energy compared to nano-$ZnWO_4$ [45]. Such blue-shift can be explained by a difference in the relaxation of WO_6 octahedra in the two tungstates, which is directly evidenced by our W L_3-edge EXAFS data (Fig. 3).

Radial distribution functions $G(R)$ for Ni/Zn–O and W–O bonds in microcrystalline and nanocrystalline $Ni(Zn)WO_4$ are shown in Fig. 3. The shape of the RDFs confirms unambiguously that the WO_6 octahedra in both tungstates are strongly distorted. The relaxation of the first shell WO_6 and $Ni(Zn)O_6$ octahedra in nanocrystalline $Ni(Zn)WO_4$ is clearly observed. Note that in the case of WO_6 octahedra the relaxation affects both shortest (at 1.8–1.9 Å) and longest (at 2.1–2.2 Å) W–O bonds. The nearest group of the W–O bonds relaxes stronger in $NiWO_4$ (by ~0.07 Å) than in $ZnWO_4$ (by ~0.02 Å), thus being responsible for a difference in the position of the photoluminescence bands in the two nanotungstates.

Finally, we would like to note that no significant temperature effect has been observed on the photoluminescence spectra of microcrystalline and nanocrystalline $NiWO_4$ in the temperature range 7–80 K. Also the photoluminescence spectra of micro-$NiWO_4$ at $T = 80$ K show weak dependence on the excitation wavelength (4.96 or 13.8 eV).

Excitation spectra

The excitation spectra of microcrystalline $NiWO_4$ show some temperature dependence in the range from 7 to 80 K due to the lattice expansion (left panel in Fig. 2). They differ from that for $ZnWO_4$ from [32] due to the difference of about 1 eV in the band gaps: $E_g = 3.6$ eV [46] for $NiWO_4$, but $E_g = 4.6$ eV for $ZnWO_4$ [47]. As a result, the strong excitonic band clearly visible at ~4.5 eV for $ZnWO_4$ [32] is not observed in the present data for $NiWO_4$ due to the spectrometer range limitations: the excitonic band is expected to be located below 3.7 eV.

The interpretation of the excitation spectra can be done using the electronic band structure diagram calculated for

$NiWO_4$ in Ref. 22 using the first-principles spin-polarized periodic linear combination of atomic orbital (LCAO) method. The valence band of $NiWO_4$ is dominated by oxygen $2p$-states hybridized with nickel $3d(t_{2g}, e_g\uparrow)$-states, whereas tungsten $5d$-states and nickel $3d(e_g\downarrow)$-states contribute largely into the bottom of conduction band [22].

The broad bands at 5–6, 8–10, 12, 13.5 and 16 eV are due to the one-electron transitions (arrows in the right panel of Fig. 2) from the top of the valence band. These transitions are even more pronounced in the case of nano-$NiWO_4$ due to quasi-localized nature of the involved electronic states. Note that such transitions have been also observed previously in nano-$ZnWO_4$ [32].

Conclusions

Microcrystalline and nanocrystalline $NiWO_4$ powders were studied by UV-VUV synchrotron radiation spectroscopy in comparison with isomorphous $ZnWO_4$ tungstate. The photoluminescence and excitation spectra were interpreted using the results of the first-principles LCAO calculations [22] and the local structural information from the Ni(Zn) K-edge and W L_3-edge x-ray absorption spectroscopy studies.

Similar to the case of $ZnWO_4$ [42,43], the photoluminescence spectra of both microcrystalline and nanocrystalline $NiWO_4$ powders originate in the $[WO_6]^{6-}$ molecular complex. However, their intensity is strongly modulated by the optical absorption of Ni^{2+} ions (intra-ion d–d transitions). In nano-$NiWO_4$, the photoluminescence band maximum is shifted to shorter wavelengths due to the strong relaxation of WO_6 octahedra.

The excitation spectra are similar in microcrystalline and nanocrystalline $NiWO_4$ powders. They consist of a number of bands due to the one-electron transitions across the band gap from the top of the valence band to the electron states in the conduction band and above. The bands are more pronounced in nano-$NiWO_4$ due to quasi-localized character of the involved electronic states.

Acknowledgments

This work was supported by Latvian Science Council Grant No. 187/2012. The experiments at DESY leading to these results have received funding from the European Community's Seventh Framework Programme (FP7/2007-2013) under grant agreement No. 226716. V.P. acknowledges the financial supports from Oulu University Strategic Funding and Research Council for Natural Sciences of the Academy of Finland.

1. B.I. Kidyarov and V.V. Atuchin, *Ferroelectrics* **444**, 144 (2013).
2. V.A. Isupov, *Ferroelectrics* **322**, 83 (2005).
3. P. Lecoq, I. Dafinei, E. Auffray, M. Schneegans, M.V. Korzhik, O.V. Missevitch, V.B. Pavlenko, A.A. Fedorov, A.N. Annenkov, V.L. Kostylev, and V.D. Ligun, *Nucl. Instrum. Methods Phys. Res. A* **365**, 291 (1995).
4. M. Kobayashi, M. Ishii, Y. Husuki, and H. Yahag, *Nucl. Instrum. Methods Phys. Res. A* **333**, 429 (1993).
5. V. Nagirnyi, A. Kotlov, L. Jönsson, M. Kirm, and A. Lushchik, *Nucl. Instrum. Methods Phys. Res. A* **537**, 61 (2005).
6. V. Nagirnyi, M. Kirm, A. Kotlov, A. Lushchik, and L. Jönsson, *J. Lumin.* **102–103**, 597 (2003).
7. V. Nagirnyi, E. Feldbach, L. Jönsson, M. Kirm, A. Kotlov, A. Lushchik, L.L. Nagornaya, F. Savikhin, and G. Svensson, *Rad. Meas.* **33**, 601 (2001).
8. E. Feldbach, L. Jönsson, M. Kirm, A. Kotlov, A. Lushchik, V. Nagirnyi, G. Svensson, and M. Åsberg-Dahlborg, *J. Lumin.* **87–89**, 1213 (2000).
9. D. Millers, S. Chernov, L. Grigorjeva, A. Popov, E. Auffray, I. Dafinei, P. Lecoq, and M. Schneegans, *J. Lumin.* **72–74**, 693 (1997).
10. D. Millers, L. Grigorjeva, S. Chernov, A. Popov, P. Lecoq, and E. Auffray, *Phys. Status Solidi B* **203**, 585 (1997).
11. F.J. Gil-Llambias, H. Rodriguez, I. Bouyssiers, M. Escudey, and I. Carkovic, *J. Catal.* **102**, 37 (1986).
12. B. Scheffer, P. Molhoek, and J.A. Moulijn, *Appl. Catal.* **46**, 11 (1989).
13. R.A. Diaz-Real, R.S. Mann, and I.S. Sambi, *Ind. Eng. Chem. Res.* **32**, 1354 (1993).
14. D.L. Stern and R.K. Grasselli, *J. Catal.* **167**, 570 (1997).
15. A.K. Bhattacharya, R.G. Biswas, and A. Hartridge, *J. Mater. Sci.* **32**, 353 (1997).
16. V. Dusastre and D.E. Williams, *J. Mater. Chem.* **9**, 965 (1999).
17. P.S. Pandey, N.S. Bhave, and R.B. Kharat, *Electrochim. Acta* **51**, 4659 (2006).
18. A.L.M. de Oliveira, J.M. Ferreira, M.R.S. Silva, G.S. Braga, L.E.B. Soledade, M.A.M.M. Aldeiza, C.A. Paskocimas, S.J.G. Lima, E. Longo, A.G. de Souza, and I.M.G. dos Santos, *Dyes Pigments* **77**, 210 (2008).
19. R.C. Pullar, S. Farrah, and N.McN. Alford, *J. Eur. Ceram. Soc.* **27**, 1059 (2007).
20. A. Kuzmin, J. Purans, R. Kalendarev, D. Pailharey, and Y. Mathey, *Electrochim. Acta* **46**, 2233 (2001).
21. S.V. Green, A. Kuzmin, J. Purans, C.G. Granqvist, and G.A. Niklasson, *Thin Solid Films* **519**, 2062 (2011).
22. A. Kuzmin, A. Kalinko, and R.A. Evarestov, *Centr. Eur. J. Phys.* **9**, 502 (2011).
23. H. He, *Int. J. Mat. Res.* **101**, 386 (2010).
24. G. Zimmerer, *Rad. Meas.* **42**, 859 (2007).
25. M. Kirm, E. Feldbach, T. Kärner, A. Lushchik, Ch. Lushchik, A. Maaroos, V. Nagirnyi, and I. Martinson, *Nucl. Instrum. Methods B* **141**, 431 (1998).
26. S. Nakonechnyi, T. Karner, A. Lushchik, C. Lushchik, V. Babin, E. Feldbach, I. Kudryavtseva, P. Liblik, L. Pung, and E. Vasil'chenko, *J. Phys.: Condens. Matter* **18**, 379 (2006).
27. A.I. Popov, L. Shirmane, V. Pankratov, A. Lushchik, A. Kotlov, V.E. Serga, L.D. Kulikova, G. Chikvaidze, and J. Zimmermann, *Nucl. Instrum. Methods B* **310**, 23 (2013).

28. P.V. Savchyn, V.V. Vistovskyy, A.S. Pushak, A.S. Voloshinovskii, A.V. Gektin, V. Pankratov, and A.I. Popov, *Nucl. Instrum. Methods B* **274**, 78 (2012).
29. V. Pankratov, A.I. Popov, L. Shirmane, A. Kotlov, G.A. Bizarri, A. Burger, P. Bhattacharya, E. Tupitsyn, E. Rowe, V.M. Buliga, and R.T. Williams, *Radiat. Meas*. **56**, 13 (2013).
30. E. Shablonin, A.I. Popov, A. Lushchik, A. Kotlov, and S. Dolgov, *Physica B* **477**, 133 (2015).
31. E.V. Savchenko, G. Zimmerer, and V.E. Bondybey, *J. Lumin*. **129**, 1866 (2009).
32. A. Kalinko, A. Kotlov, A. Kuzmin, A. Pankratov, A.I. Popov, and L. Shirmane, *Centr. Eur. J. Phys*. **9**, 432 (2011).
33. N.B. Gruzdev, V.I. Sokolov, V.A. Pustovarov, and V.N. Churmanov, *Fiz. Nizk. Temp.* **41**, 285 (2015) [*Low Temp. Phys*. **41**, 218 (2015)].
34. A. Kuzmin, *Physica B* **208–209**, 175 (1995).
35. V.L. Aksenov, M.V. Kovalchuk, A.Yu. Kuzmin, Yu. Purans, and S.I. Tyutyunnikov, *Crystallogr. Rep*. **51**, 908 (2006).
36. A. Kuzmin and J. Purans, *J. Phys.: Condens. Matter* **12**, 1959 (2000).
37. A. Anspoks, A. Kalinko, J. Timoshenko, and A. Kuzmin, *Solid State Commun*. **183**, 22 (2014).
38. A.L. Ankudinov, B. Ravel, J.J. Rehr, and S.D. Conradson, *Phys. Rev. B* **58**, 7565 (1998).
39. J.J. Rehr and R.C. Albers, *Rev. Mod. Phys*. **72**, 621 (2000).
40. H. Weitzel, *Z. Kristallogr.* **144**, 238 (1976).
41. A. Kuzmin and J. Purans, *Rad. Meas.* **33**, 583 (2001).
42. V.N. Kolobanov, I.A. Kamenskikh, V.V. Mikhailin, I.N. Shpinkova, D.A. Spassky, B.I. Zadneprovsky, L.I. Potkin, and G. Zimmerer, *Nucl. Instrum. Methods Phys. Res. A* **486**, 496 (2002).
43. V. Nagirnyi, E. Feldbach, L.J¨onson, M. Kirm, A. Lushchik, V.A. Nefedov, and B.I. Zadneprovski, *Nucl. Instrum. Methods Phys. Res. A* **486**, 395 (2002).
44. L.N. Limarenko, A.E. Nosenko, M.V. Pashkovskii, and D.L.L. Futorskii, *Influence of Structural Defects on Physical Properties of Tungstates*, Vysha Shkola, Lvov (1978).
45. A. Kalinko and A. Kuzmin, *J. Lumin*. **129**, 1144 (2009).
46. T. Ejima, T. Banse, H. Takatsuka, Y. Kondo, M. Ishino, N. Kimura, M. Watanabe, and I. Matsubara, *J. Lumin*. **119–120**, 59 (2006).
47. A. Kalinko, A. Kuzmin, and R.A. Evarestov, *Solid State Commun*. **149**, 425 (2009).